

## Competing sigmatropic shift rearrangements in excited allyl radicals

D. Stranges,<sup>1,2,a)</sup> P. O’Keeffe,<sup>1</sup> G. Scotti,<sup>1</sup> R. Di Santo,<sup>3</sup> and P. L. Houston<sup>4</sup>

<sup>1</sup>Dipartimento di Chimica, Università “La Sapienza,” P.le A. Moro 5, Rome I-00185, Italy

<sup>2</sup>ISMN-CNR, Sez. Roma I, P.le A. Moro 5, Rome I-00185, Italy

<sup>3</sup>Dipartimento di Studi Farmaceutici, Università “La Sapienza,” P.le A. Moro 5, 00185 Rome, Italy

<sup>4</sup>School of Chemistry and Biochemistry, Georgia Institute of Technology, Atlanta, Georgia 30332, USA

(Received 7 December 2007; accepted 18 March 2008; published online 16 April 2008)

The competition between rearrangement of the excited allyl radical via a 1,3 sigmatropic shift versus sequential 1,2 shifts has been observed and characterized using isotopic substitution, laser excitation, and molecular beam techniques. Both rearrangements produce a 1-propenyl radical that subsequently dissociates to methyl plus acetylene. The 1,3 shift and 1,2 shift mechanisms are equally probable for  $\text{CH}_2\text{CHCH}_2$ , whereas the 1,3 shift is favored by a factor of 1.6 in  $\text{CH}_2\text{CDCH}_2$ . The translational energy distributions for the methyl and acetylene products of these two mechanisms are substantially different. Both of these allyl dissociation channels are minor pathways compared to hydrogen atom loss. © 2008 American Institute of Physics. [DOI: 10.1063/1.2907714]

Rearrangement reactions form a broad class of transformations of enormous importance in chemical synthesis. The 1,2-sigmatropic shift rearrangement has been known since 1838 (Ref. 1) and was reviewed as early as 1932.<sup>2</sup> Although the most common shift rearrangements in organic synthesis involve cations, rearrangements of radicals are also prevalent and important in combustion, photochemistry, and atmospheric chemistry.<sup>3,4</sup> Yet compared to rearrangements for cations, or even anions, little is understood about the competition in radicals between different rearrangement channels.

In this communication we report observation of three competing channels in the dissociation of the allyl radical ( $\text{C}_3\text{H}_5$ ) excited to a level with 115 kcal/mol in energy. The first channel involves a simple C–H cleavage, while the other two channels involve isotopically distinguishable sigmatropic shift rearrangements followed by C–C cleavage. Use of molecular beam and laser photolysis techniques coupled with selective deuterium substitution has allowed us to determine the branching ratio between the two rearrangement channels. The ratio is in reasonable agreement with Rice-Ramsperger-Kassel-Marcus (RRKM) calculations based on *ab initio* potential energy surfaces.

The allyl radical has received substantial recent attention due to its importance in combustion and atmospheric chemistry.<sup>5–7</sup> Its spectroscopy has been detailed by several studies,<sup>8–11</sup> and its photodissociation has been examined both by sophisticated laser techniques<sup>12</sup> and by molecular beam methods.<sup>13,14</sup> Following excitation to the  $\text{C}(^2B_1)$  electronic state, internal conversion takes place in about 22 ps [Ref. 12(c)] and is followed by dissociation on the ground electronic surface to give principally hydrogen atom loss. A secondary channel, observed in earlier molecular beam measurements,<sup>13</sup> leads to methyl radicals plus acetylene. Quantum mechanical calculations have also been performed both on the allyl dissociation and on the methyl plus acetylene reverse reaction.<sup>12,15,16</sup> The former show that the methyl

elimination channel can occur by two mechanisms, each of which produces the 1-propenyl radical as an intermediate.

In the current experiments allyl iodide/ $d_1$  allyl iodide was entrained at 0.2% in a stream of helium and pyrolyzed in a pulsed nozzle<sup>17</sup> attached to the rotating source of a molecular beam apparatus.<sup>18</sup> The allyl radicals were excited with excimer laser light at 248 nm at a location 38.8 cm from a detector that consist of a electron impact ionization region, a quadrupole mass spectrometer, and a “door knob” detector assembly. The arrival time distribution of product ions was recorded at different laboratory angles. Conservation of energy and linear momentum allowed measurement of the product translational energy distributions, which made it possible to measure the branching ratios for different channels.

The major observed channel for allyl dissociation involves hydrogen loss, while the interesting channels in the current context are the two mechanisms that produce methyl and acetylene. A computational study (discussed below in more detail) on all of the possible isomerization and dissociation channels of both the  $\text{C}_3\text{H}_5$  and  $\text{C}_3\text{H}_4\text{D}$  systems has been performed; however, only the energies and geometries of the species pertaining to the H/D atom shift mechanisms and carbon-carbon bond breaking channels are reported in this communication. The potential energy diagram for the  $\text{C}_3\text{H}_4\text{D}$  system and the relevant structures are shown in Fig. 1. The two competing reactions discussed in this study are indicated by the arrows where reactions proceeding towards the right-hand side of the figure [reaction (1)] take place via a 1,3 shift followed by formation of  $\text{DCCH} + \text{CH}_3$ , while those proceeding towards the left-hand side of this figure [reaction (2)] take place via two sequential 1,2 shifts and subsequent dissociation to  $\text{HCCH} + \text{CH}_2\text{D}$ .

Figure 2 shows the arrival time distributions (ATDs) for  $m/e=27$  and  $m/e=26$  ions as well as the translational energy distributions [ $P(E)$ ’s] for the two product channels. The ATD of the ions is a result of the neutral flight time of the photo-fragments from the interaction region to the ionizer plus the ion flight time from the ionizer to the detector. The ATD of

<sup>a)</sup>Electronic mail: domenico.stranges@uniroma1.it.

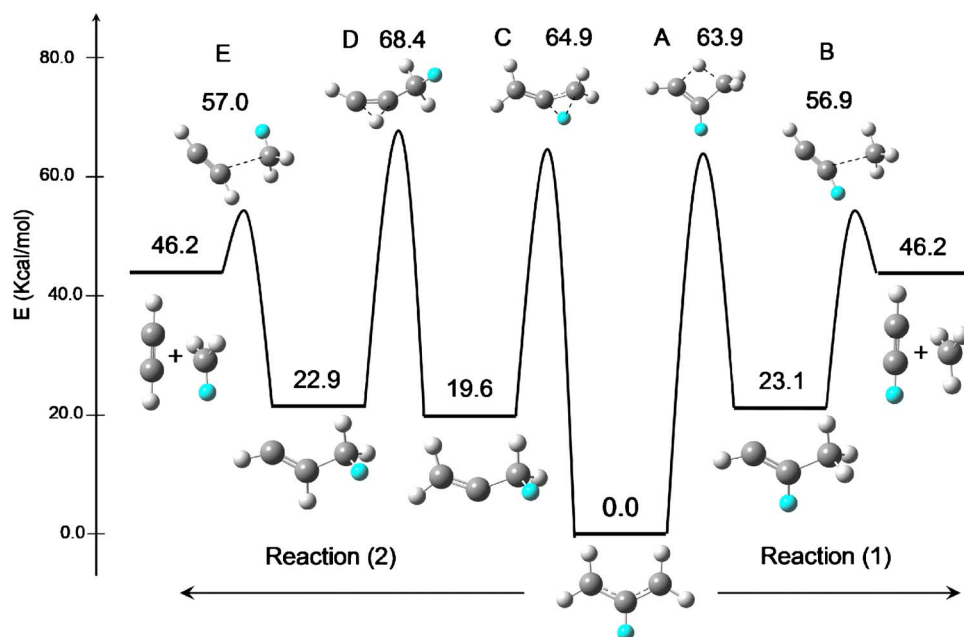


FIG. 1. (Color online) Potential energy barriers describing the 1,2 and 1,3 H/D atom shift mechanisms and carbon-carbon bond breaking channels in the  $\text{CH}_2\text{CDCH}_2$  system. The barriers heights, stable structure energies, and geometries were calculated at the QCISD(T)/cc-pVTZ//B3LYP/cc-pVDZ with zero point energy (ZPE) corrections by a B3LYP/cc-pVDZ anharmonic frequency analysis.

the  $m/e=27$  ions results exclusively from ionization of the DCCH photofragments [formed in reaction (1)] in the ionizer. Simulating this distribution allowed the  $P(E)$  of reaction (1) to be extracted (full line in the bottom panel of Fig. 2). On the other hand, the  $m/e=26$  ion ATD contains two contributions: one due to the ionization of the HCCH fragments [from reaction (2)] and a second contribution (red full line) due to the dissociative ionization of the DCCH fragments to  $\text{DCC}^+$  ions in the ionizer. In this case, the simulation is performed using the  $P(E)$  of reaction (1) obtained above and by varying the relative intensity and the shape of the translational energy distribution of reaction (2) until the best fit of this ion ATD is achieved. The resulting  $P(E)$  for reaction (2) is shown as a dotted line in the bottom panel of Fig. 2. The  $P(E)$  of the hydrogen loss channel (not shown) has its peak close to 0 kcal/mol, with an average translational energy of 6 kcal/mol. The resulting kinetic energy of the heavy fragments of this channel is not sufficient to give a contribution to the flight time distributions measured at a laboratory angle of  $15^\circ$ , and therefore no signal due to dissociative ionization of these fragments is observed in Fig. 2.

RRKM calculations show that the reverse isomerization reactions for 1- and 2-propenyl radicals (i.e., reverse reactions over transition states A, C, and D of Fig. 1) are much slower than the dissociation reactions, and therefore measurement of either the  $\text{CH}_3/\text{CH}_2\text{D}$  ratio or the  $\text{DCCH}/\text{HCCH}$  ratio gives the branching ratio of process (1) to process (2). In this work the  $\text{DCCH}/\text{HCCH}$  ratio was obtained by measuring the arrival time distributions for the  $m/e=27, 26, 25, 24, 14, 13$ , and 12 ions at a laboratory angle of  $15^\circ$  and simulating each of the distributions using the  $P(E)$ 's for reactions (1) and (2). The relative contribution of these two  $P(E)$ 's to each of these ion arrival time distributions, once integrated over the recoil velocity and angle and corrected for the kinematics, yields the relative contribution of the DCCH and HCCH channels to each ion arrival distribution. Normalizing for the number of counts in each ion channel then gives the dissociative ionization pattern of these

two photofragments. Finally summing over all ion yields gives the branching ratio of process (1) to process (2). The ratio found in this way was  $\text{BR}_D=(1):(2)=1.6 \pm 0.1$ . It should be noted that the above distributions were measured following photodissociation by an unpolarized laser. This choice can be justified by the fact that a previous study showed that the angular distribution of fragments formed in

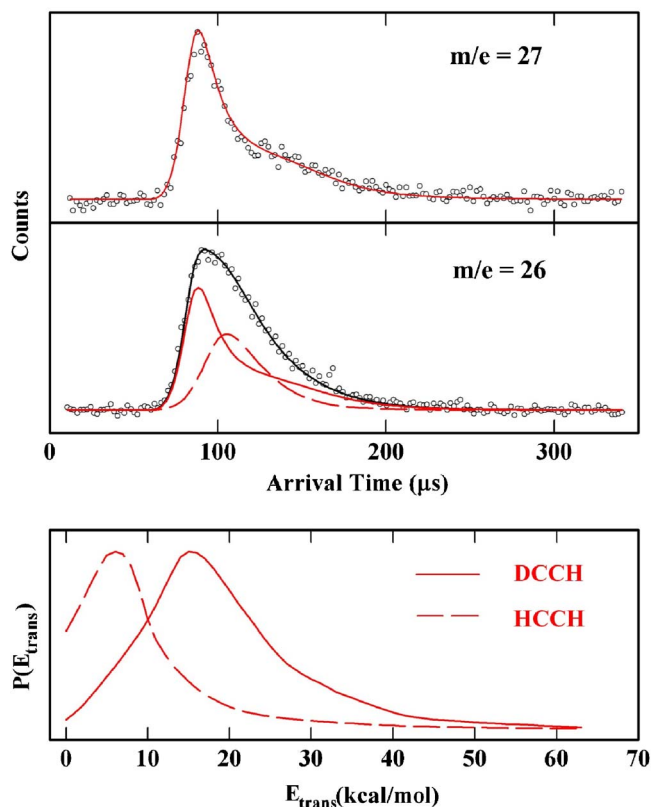


FIG. 2. (Color online) Arrival time distributions for DCCH and HCCH (recorded at  $m/e=27$  and 26, respectively) taken at a laboratory angle of  $15^\circ$  (top two panels). Translational energy distributions for the 1,3 (solid) and 1,2 (dashed) shift channels (bottom panel).

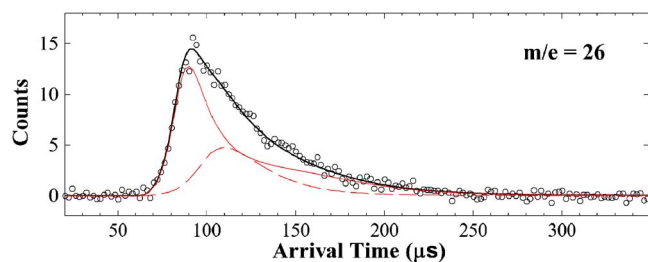


FIG. 3. (Color online) Arrival time distribution of  $m/e=26$  ions taken at a laboratory angle of  $15^\circ$  following photodissociation of the  $\text{H}_2\text{CCHCH}_2$  radical. The full line shows the contribution of the process, 1 while the dotted line shows that of process 2. The  $P(E)$ 's used in the simulations are those shown in Fig. 2.

the photodissociation of the methyl plus acetylene channel is isotropic, i.e.,  $\beta=10$ .<sup>13</sup>

The branching ratio  $\text{BR}_\text{H}$  for the nondeuterated allyl has been obtained by simulating the HCCH arrival time distributions from photodissociation of  $\text{C}_3\text{H}_5$  using the  $P(E)$ 's determined for processes (1) and (2) in the photodissociation of  $\text{C}_3\text{H}_4\text{D}$ . Varying their relative contributions, in order to obtain the best fit, yielded  $\text{BR}_\text{H}=(1):(2)=1.0 \pm 0.1$ . The resulting simulation of the ATD of the  $m/e=\text{HCCH}^+$  ions, recorded following the photodissociation of the nondeuterated radical at a laboratory angle of  $15^\circ$ , is shown in Fig. 3. The ATD of the momentum matched  $m/e=15$  ( $\text{CH}_3$ ) fragments was also detected in this case. The  $P(E)$ 's shown in Fig. 2 simulated this distribution very well, demonstrating that the  $m/e=26$  fragments were indeed produced by photolysis of the  $\text{C}_3\text{H}_5$  and not from a contamination in the beam.

*Ab initio* calculations have been performed, using the GAUSSIAN03 package,<sup>19</sup> on the energies and vibrational frequencies of the stable and transition state structures shown in Fig. 1. These structures were optimized at the B3LYP/cc-pVDZ level,<sup>20,21</sup> followed by single point electronic energy calculations at the QCISD(T)/cc-pVTZ level<sup>21,22</sup> and zero point energy (ZPE) corrections by a B3LYP/cc-pVDZ anharmonic frequency analysis.<sup>21,23</sup> For the undeuterated system the following barrier heights were obtained:  $A \sim 63.9$ ,  $B \sim 56.8$ ,  $C \sim 64.3$ ,  $D \sim 67.8$ , and  $E \sim 56.8$  (in kcal/mol with respect to  $\text{CH}_2\text{CHCH}_2$ ); while for the deuterated system the corresponding barrier heights were  $A \sim 63.9$ ,  $B \sim 56.9$ ,  $C \sim 64.9$ ,  $D \sim 68.4$ , and  $E \sim 57.0$  (in kcal/mol with respect to  $\text{CH}_2\text{CDCH}_2$ ). The different barrier heights in the two systems are due to the differing ZPEs. The possibility of dissociation to the vinylidene plus methyl products has not been considered in these calculations due to the fact that previous high level *ab initio* calculations showed that the difference in energy between acetylene and vinylidene was 44.0 kcal/mol.<sup>24</sup> Therefore even in the absence of a barrier to dissociation, the asymptotic energy of this channel in the case of the nondeuterated radical is at least 22.4 kcal/mol higher than the barrier to the 1,2 H atom shift mechanism, indicating that a statistical dissociation by direct carbon-carbon bond breaking from 2-propenyl to  $\text{H}_2\text{CC}+\text{CH}_3$  is negligible with respect to the 1,2 H atom shift reaction.

The energies, geometries, and vibrational frequencies obtained from the above *ab initio* calculations were then used as input for RRKM calculations<sup>25,26</sup> to investigate the

microcanonical reaction rates. The rates calculated in this way allowed the branching ratios to be calculated by a full integration of the forward rate equations, including the H-loss reactions. In this RRKM model the density and sum of states of the stable species and transition states, respectively, were calculated using the direct count method<sup>27</sup> in which the torsional modes involving  $\text{CH}_3$  and  $\text{CH}_2\text{D}$  were treated using the hindered internal rotor model of Barker and Shovlin,<sup>28</sup> while all of the other vibrations were modeled by harmonic oscillators. The predicted branching ratio for the undeuterated system is  $\text{BR}_\text{H}=9.6$ , larger than our measurement of 1.0, while that of the deuterated system is  $\text{BR}_\text{D}=16.5$ . However, as the calculated values for the barrier heights are likely to be accurate to no more than  $\pm 2-3$  kcal/mole, it is reasonable to modify the barriers within these limits in order to obtain better agreement with experiment. Indeed, increasing the energy of barrier A by 3 kcal/mol and decreasing those of reactions C and D by 2 kcal/mol brings the calculated ratios  $\text{BR}_\text{H}$  and  $\text{BR}_\text{D}$  to 2.2 and 3.76, respectively, which are much closer to the measured values.

The branching ratio  $\text{BR}_\text{D}$  for deuterated allyl is larger due to the kinetic isotope effect (KIE), which leaves channel (1) nearly unchanged while decreasing the yield of channel (2). Assuming a KIE of unity for channel (1), where the deuterium is not directly involved in the reaction, then  $\text{BR}_\text{D}/\text{BR}_\text{H}=[(1):(2)]_\text{D}/[(1):(2)]_\text{H}=(2)_\text{H}/(2)_\text{D}=\text{KIE}$ . From the measured values of  $\text{BR}_\text{D}$  and  $\text{BR}_\text{H}$ , we find  $\text{KIE}=1.6$ , which is in excellent agreement with our calculated value of 1.7 using rate constants from RRKM results. It should be noted that the calculated value of this ratio remains unchanged on modification of the barrier heights, showing that the isotope effect is very consistently reproduced by the theory. This result indicates that the KIE is due to the changes in the ZPEs and the changes in the sums and densities of states resulting from deuteration. At the high energies involved in this experiment it appears that the contribution of tunneling (not taken into account in the RRKM model) is minimal. The branching to the major H-loss channel is calculated to be 97.9%, close to our measured value of 95% based on the nondeuterated compound.

The possible effect of scrambling (interchange of the H and D atoms in the allyl radical) was investigated by means of RRKM calculations. The scrambling is due to (i) the reverse reaction over barrier C and (ii) the ring closure to form the cyclopropyl radical followed by a 1,2 H-atom shift and ring reopening. The calculations gave a total yield of less than 0.2% for these two processes and therefore they have a negligible effect on the measured ratios. This conclusion is supported by the experimental observation of significantly different  $P(E)$ 's (due to different dynamics) for the two reactions, whereas extensive scrambling would have led to similar distributions. It should be noted that by examining Fig. 1 and the  $P(E)$ 's in Fig. 2, it would appear that the peak in the  $P(E)$  for reaction (2) (7 kcal/mol) corresponds to the reverse barrier height between TS E and the  $\text{C}_2\text{H}_2+\text{CH}_2\text{D}$  products, while the  $P(E)$  of the reaction (1) (15 kcal/mol) corresponds to the difference between the barrier height of TS A and the  $\text{C}_2\text{HD}+\text{CH}_3$  products. A detailed discussion of

these nonstatistical dynamics is not within the scope of this communication and will be discussed in detail in a forthcoming paper.<sup>29</sup>

In summary, for dissociation of the allyl radical these measurements show that both the 1,3 and sequential 1,2 shift mechanisms are important. It seems likely from these results that such competition between mechanisms giving the same products takes place in other radical rearrangement processes. To the best of our knowledge such competing 1,2 and 1,3 H-atom shift mechanisms or even the 1,3 shift mechanism alone have not previously been observed experimentally in any small hydrocarbon molecule under well-defined conditions.<sup>30</sup>

This research was supported by the Italian Ministero dell'Università e della Ricerca (MUR, PRIN 2005), a Marie Curie Intra-European Fellowship within the Sixth European Community Framework Programme (Contract No. MEIF-CT-2005-024895). Acknowledgment is made to the Donors of The American Chemical Society Petroleum Research Fund for the partial support of this work (No. 46303-AC6). We are thankful to B. K. Carpenter for helpful discussions.

<sup>1</sup>J. von Liebig, *Ann. Chem.* **25**, 27 (1838).

<sup>2</sup>F. C. Whitmore, *J. Am. Chem. Soc.* **54**, 3274 (1932).

<sup>3</sup>J. W. Wilt, in *Free Radicals*, edited by J. K. Kochi (Wiley, New York, 1973).

<sup>4</sup>D. C. Nonhebel and J. C. Walton, in *Free-Radical Chemistry; Structure and Mechanism* (Cambridge University Press, London, 1974).

<sup>5</sup>J. M. Tulloch, M. T. Macpherson, C. A. Morgan, and M. J. Pilling, *J. Phys. Chem.* **86**, 3812 (1982).

<sup>6</sup>R. X. Fernandes, B. R. Giri, H. Hippler, C. Kachiani, and F. Striebel, *J. Phys. Chem. A* **109**, 1063 (2005); T. Bentz, B. R. Giri, H. Hippler, M. Olzmann, F. Striebel, and M. Szöri, *J. Phys. Chem. A* **111**, 3812 (2007).

<sup>7</sup>M. E. Jenkin, T. P. Murrells, S. J. Shalliker, and G. D. Hayman, *J. Chem.*

*Soc., Faraday Trans.* **89**, 433 (1993).

<sup>8</sup>A. D. Sappay and J. C. Weisshaar, *J. Phys. Chem.* **91**, 3731 (1987).

<sup>9</sup>D. W. Minsek and P. Chen, *J. Phys. Chem.* **97**, 13375 (1993).

<sup>10</sup>J.-C. Wu, R. Li, and J.-L. Chang, *J. Chem. Phys.* **113**, 7286 (2000).

<sup>11</sup>C.-W. Liang, C.-C. Chen, C.-Y. Wei, and Y.-T. Chen, *J. Chem. Phys.* **116**, 4162 (2002).

<sup>12</sup>(a) H.-J. Deyerl, T. Gilbert, I. Fischer, and P. Chen, *J. Chem. Phys.* **107**, 3329 (1997); (b) I. Fischer and P. Chen, *J. Phys. Chem. A* **106**, 4291 (2002); (c) T. Schultz and I. Fischer, *J. Chem. Phys.* **107**, 8197 (1997); (d) H.-J. Deyerl, I. Fischer, and P. Chen, *J. Chem. Phys.* **110**, 1450 (1999).

<sup>13</sup>D. Stranges, M. Stemmler, X. Yang, J. D. Chesko, A. G. Suits, and Y. T. Lee, *J. Chem. Phys.* **109**, 5372 (1998).

<sup>14</sup>D. E. Szpunar, M. L. Morton, and L. J. Butler, *J. Phys. Chem. B* **106**, 8086 (2002); D. E. Szpunar, Y. Liu, M. J. McCullagh, and L. J. Butler, *J. Chem. Phys.* **119**, 5078 (2003).

<sup>15</sup>S. G. Davis, C. K. Law, and H. Wang, *J. Phys. Chem. A* **103**, 5889 (1999).

<sup>16</sup>R. Gomez-Galderas, M. L. Coote, D. J. Henry, and L. Radom, *J. Phys. Chem. A* **108**, 2874 (2004).

<sup>17</sup>H. Clauberg, D. W. Minsek, and P. Chen, *J. Am. Chem. Soc.* **114**, 99 (1992).

<sup>18</sup>The apparatus in Rome is very similar to that described in A. M. Wodtke and Y. T. Lee, *J. Phys. Chem.* **89**, 4744 (1985).

<sup>19</sup>M. J. Frisch, G. W. Trucks, H. B. Schlegel *et al.*, GAUSSIAN 03, Revision B. 01, M. J. Frisch, Gaussian Inc., Pittsburgh PA 2003.

<sup>20</sup>A. D. Becke, *J. Chem. Phys.* **97**, 9173 (1992).

<sup>21</sup>T. H. Dunning, *J. Chem. Phys.* **90**, 1007 (1989).

<sup>22</sup>J. A. Pople, M. Head-Gordon, and K. Raghavachari, *J. Chem. Phys.* **87**, 5968 (1987).

<sup>23</sup>V. Barone, *J. Chem. Phys.* **122**, 014108 (2005).

<sup>24</sup>S. Zhou and J. M. Bowman, *Chem. Phys. Lett.* **368**, 421 (2003).

<sup>25</sup>J. R. Barker, *Int. J. Chem. Kinet.* **33**, 232 (2001).

<sup>26</sup>R. G. Gilbert and S. C. Smith, *Theory of Unimolecular and Recombination Reactions* (Blackwell Scientific, Oxford, 1990).

<sup>27</sup>S. E. Stein and B. S. Rabinovitch, *J. Chem. Phys.* **58**, 2438 (1973).

<sup>28</sup>J. R. Barker and C. N. Shovlin, *Chem. Phys. Lett.* **383**, 203 (2004).

<sup>29</sup>P. O'Keeffe, G. Scotti, P. L. Houston, and D. Stranges (unpublished).

<sup>30</sup>E. Chamorro, J. C. Santos, B. Gomez, R. Contreras, and P. Fuentealba, *J. Phys. Chem. A* **106**, 11533 (2002).